Thermal Stability of Ultrathin Amorphous Carbon Films for Energy-Assisted Magnetic Recording

N. Wang and K. Komvopoulos
Department of Mechanical Engineering, University of California, Berkeley, California 94720

Abstract

Energy-assisted magnetic recording (EAMR) uses a laser-optical system integrated into the magnetic head to heat locally a fine-grained material of high magnetic anisotropy energy density above its Curie temperature, to store single bits in very small areas without being limited by the superparamagnetic effect. However, localized laser heating may affect the thermal stability of the carbon overcoat of the hard disk. To examine the effect of laser heating on the overcoat thermal stability, ultrathin amorphous carbon (*a*-C) films of similar thickness (~3.6 nm) synthesized by filtered cathodic vacuum arc (FCVA) and chemical vapor deposition (CVD) were subjected to repetitive heating under different laser powers. Carbon hybridization and surface roughness of the *a*-C films were examined by Raman spectroscopy and atomic force microscopy, respectively. For the laser power range examined (150–300 mW), *a*-C films produced by the FCVA technique demonstrated greater thermal stability than CVD films of similar thickness. To investigate the possibility of further reducing the magnetic spacing, thinner (~0.9 nm) *a*-C films deposited by the FCVA method were subjected to the same laser heating conditions. Although the thermal stability of the FCVA-synthesized *a*-C films exhibited thickness dependence, even the thinner (~0.9 nm) FCVA film demonstrated higher thermal stability than the much thicker (~3.6 nm) CVD film. The results of this study illustrate the high potential of FCVA as a coating method for EAMR.

Index Terms—Amorphous carbon, atomic force microscopy, carbon atom hybridization, energy-assisted magnetic recording, filtered cathodic vacuum arc, Raman spectroscopy, thermal stability, ultrathin films

---

Published in *IEEE Transactions on Magnetics*, Vol. 47, No. 9, 2011, pp. 2277–2282.

I. INTRODUCTION

Storage technology breakthroughs such as the advent of the giant magneto-resistive head and recent advances in thin-film deposition techniques have led to dramatic increases in the magnetic storage area density of hard-disk drives [1]. Despite rapid evolutions in storage technologies, continuously increasing demands for larger storage capacities and lower production cost have raised the storage density barrier to levels on the order of 10 Tb/in^2 [2]. However, such high storage densities cannot be currently achieved because of fundamental problems associated with magnetic particle instability, signal-to-noise ratio, and read/write data rate resulting from the superparamagnetic effect. Energy-assisted magnetic recording (EAMR) [3] promises to circumvent above obstacles, ultimately enabling extremely-high-density magnetic recording (EHDMR). EAMR uses the optical power of a laser beam, effectively coupled with the magnetic medium of the rotating hard disk, to rapidly heat a track of the magnetic medium above its Curie temperature. The instantaneous decrease in coercivity caused by the intense heat flux allows information to be stored in the form of single bits by the magnetic field of the read/write element embedded at the trailing edge of the recording head.

The high magnetic anisotropy of FePt alloy [4] makes it a prime candidate magnetic medium for EHDMR applications. By using a near-field transducer integrated into the magnetic head, local heating of FePt above its Curie temperature can be accomplished with a laser beam of sub-100-nm resolution and high coupling efficiency [5,6]. Because the Curie temperature of FePt nanoparticles depends strongly on their size and composition [7,8], the local temperature rise during laser heating of the FePt alloys used in EAMR disks has been reported to be about 200°C [9] and 400°C [5,7]. Therefore, it may be inferred that the temperature in the magnetic medium during laser heating should be above 227°C. However, despite the evidence that EAMR is an effective means of overcoming the superparamagnetic limit, the unknown effect of laser heating on the structural stability of the carbon overcoat is of great concern.

According to Wallace's law, the strength of a magnetic signal decays exponentially with distance. To further increase the storage density, the distance between the read/write transducer of the magnetic

head and the magnetic medium of the hard disk must be reduced below 6.5 nm [10]. To achieve this goal, the thickness of the carbon overcoat on the disk must decrease from typically ~4 nm in current hard-disk drives to ~1 nm. The effect of localized laser heating on the thermal stability of nanometer-thick carbon films is currently unknown.

Amorphous carbon (α-C) is the principal overcoat material of thin-film disks and magnetic heads, mainly because of its high hardness and excellent wear resistance. α-C films are generally characterized by varying percentages of trigonal (sp^2) and tetrahedral (sp^3) atomic carbon hybridizations. The fractions of sp^2 and sp^3 carbon–carbon bonding depend strongly on the process conditions of the particular deposition method. Elevated temperatures in EAMR may lead to stress relaxation and changes in atomic carbon hybridization [11,12], altering the α-C film composition and, in turn, degrading the corrosion and tribological properties at the head/disk interface. Therefore, the thermal stability of α-C films used as overcoats in EAMR is of paramount importance.

Previous studies dealing with the thermal stability of nanometer-thick carbon overcoats were focused on the overcoat behavior under oxygen-free environments and temperatures between 350 and 1200°C. For example, rapid annealing of carbon films synthesized from methane by ion beam deposition in a nitrogen atmosphere of ~500°C resulted in hydrogen loss and graphitic recrystallization [13]. Also, *a*-C films produced by radio-frequency plasma decomposition of acetylene exhibited thermal instability at 390°C [14]. Conversely to previous film deposition methods, tetrahedral *a*-C films deposited on Si(100) by filtered cathodic vacuum arc (FCVA) demonstrated composition stability during annealing up to 1100°C, above which, the film microstructure exhibited rapid sp^3-to-sp^2 transformation [15]. In addition to the composition stability, FCVA carbon films demonstrate stable mechanical strength over a wide temperature range. For example, the hardness and elastic modulus of FCVA-synthesized *a*-C films have been reported to remain stable during thermal heating up to temperatures as high as 850°C [16]. Although the previous studies indicate that FCVA produces thermally stable carbon films, laser heating in EAMR is localized and significantly more rapid (on the order of nanoseconds). This abrupt and localized heating

differs significantly from the uniform heating conditions encountered in annealing studies, such as those mentioned above. In addition, the *a*-C film thickness of hard disks in current disk-drives is equal to ~4 nm or less, whereas the thickness of the *a*-C films examined in previous thermal annealing studies was larger than 40 nm. Although damage due to laser heating of 4.5-nm-thick carbon overcoats deposited by sputtering has been correlated with a decrease in reflectivity, caused by the decrease in film density and surface roughening [17], changes in the overcoat nanomechanical/tribological properties were not investigated.

A review of the literature, including the studies mentioned above, indicates that knowledge of the thermal stability of ultrathin *a*-C films under localized laser heating conditions is sparse. Therefore, the main objective of this study was to examine the effect of localized laser heating on the structural stability of ultrathin *a*-C films synthesized by chemical vapor deposition (CVD) and filtered cathodic vacuum arc (FCVA). Changes in atomic carbon hybridization and surface roughness of the films were studied by visible Raman spectroscopy and atomic force microscopy (AFM), respectively. Raman and AFM results of *a*-C films possessing different thickness synthesized by CVD and FCVA are contrasted below to show which deposition process produces the most thermally stable carbon overcoats for EAMR and to elucidate the effect of film thickness on the thermal stability of *a*-C films synthesized by the FCVA method.

II. EXPERIMENTAL PROCEDURES

A. Sample Preparation

Since the focus of this study was the thermal stability of ultrathin *α*-C films for EAMR hard disks, 2.5-inch-diameter thin-film disks consisting of a glass substrate, a soft underlayer of a complex alloy for controlling the growth and enhance the adhesion of the magnetic layer to the glass substrate), a ~12-nm-thick FePt magnetic layer, and a ~4-nm-thick *a*-C overcoat deposited by CVD were used in the experiments of this study. The disks were not lubricated to avoid complications in the measurements. CVD film deposition was performed at a temperature in the range of 90–120°C, using ethylene (C_2H_4)

gas as a precursor at a flow rate of 250–300 sccm. In all of the CVD experiments, the base and working pressures were fixed at ~1×10^{-7} and 2×10^{-2} Torr, respectively.

To deposit *a*-C films on the FePt magnetic medium of similar disks by the FCVA technique, hard disks coated with CVD *a*-C films were loaded onto the substrate stage of a custom-made FCVA system [18–20], and the carbon overcoat was sputter-etched with a 500-eV Ar^+ ion beam generated by a 64-mm Kaufman ion source (Commonwealth Scientific, Alexandria, VA) under a working pressure of ~2.1×10^{-4} Torr. Under these sputter etching conditions, the CVD *a*-C film was completely removed after 2 min of Ar^+ ion bombardment, as confirmed by X-ray photoelectron spectroscopy full-spectrum scanning. After cooling down for 5 min, the substrate holder was rotated by 90° to a position normal to the carbon ion flux and *a*-C film deposition was initiated. The base pressure in the FCVA chamber was fixed at ~3×10^{-6} Torr, while the working pressure during deposition was less than 1×10^{-4} Torr. To ignite and maintain a stable arc discharge during deposition, the potential and the current between the 99.99% pure graphite cathode and the anode were kept at 24 V and 89 A, respectively. A pulsed substrate bias voltage of –100 V and 25 kHz frequency was used in all of the FCVA depositions. These FCVA process conditions resulted in a deposition rate of ~0.3 nm/s. For uniform sputter etching and deposition, the substrate holder was rotated at 60 rpm during both Ar^+ ion etching and film deposition.

Because of the thermal stability and known optical properties of silicon, p-doped Si(100) substrates coated with *a*-C films together with the exposed FePt magnetic medium of the sputtered disks were used to measure the film thickness with an ellipsometer (M-2000, J. A. Woollam Co., Lincoln, NB). The thickness of *a*-C films synthesized under identical chamber conditions and different deposition times was measured by cross-section transmission electron microscopy and was then used to calibrate the film thickness measured by ellipsometry. For comparison with the *a*-C films deposited by the CVD method and to examine the film thickness effect on thermal stability, *a*-C films of thickness equal to ~3.6 and ~0.9 nm were deposited on exposed FePt magnetic layers of hard disks under the above FCVA working conditions.

B. Laser Thermal Treatment

Each disk was mounted on a spindle rotating at 5400 rpm and was then exposed to a continuous-wave Vanadate laser beam of ~4 μm diameter and 20 W maximum power. The laser beam was traversed in the disk radial direction in increments of 9 μm per revolution, resulting in a 0.5-mm-wide annulus of partially overlapped spiral tracks. Each laser-heated annulus was subjected to 610 successive heating cycles (corresponding to total heating time of ~1 h) before it was examined with the Raman spectrometer. Due to the high rotational speed and small laser-heated spot on the disk surface, *in-situ* measurement of the temperature profile was difficult. Therefore, to obtain an approximate estimate of the temperature rise for a given laser power, a Sn dot on the disk surface was heated at various laser powers. Since melting of the Sn dot was observed at a laser power of 150 mW, it was concluded that the surface temperature rise at this laser power was higher than the melting point of Sn (232°C). In view of this finding and the fact that the temperature rise in the magnetic medium should be >227°C, the laser power in the thermal stability experiments was chosen to be in the range of 150–300 mW.

C. Microanalysis

Changes in surface properties and roughness of the laser-heated *a*-C films were qualitatively studied with an optical surface analyzer (OSA) (Candela Instruments, San Jose, CA). The entire disk surface was spirally scanned, and all laser-heated tracks were marked for subsequent AFM and Raman analysis. Surface topographies of the *a*-C films were examined with an AFM (Nanoscope III, Digital Instruments, Plainview, NY) operated in the tapping mode. AFM imaging was performed with Si tips of nominal radius of curvature <10 nm attached to microcantilevers of 5 N/m stiffness and 150 kHz resonant frequency. Images of 1×1 μm^2 areas obtained from the central region of each laser-heated annulus were used to calculate the arithmetic average roughness R_a of each film as a function of laser power. The R_a roughness of as-deposited *a*-C films was calculated from AFM images obtained from surface regions at distances equal to ~2 mm from the laser-heated annulus. Raman spectroscopy is a standard nondestructive method for studying the carbon bonding structure. Films deposited on the FePt magnetic layer of hard

disks were heated at different laser powers and their thermal stability was studied by visible Raman spectroscopy (WiRE^{TM}, Renishaw Raman Imaging Microscope, Hoffman Estate, IL) using a 514.5 nm Ar^+ ion laser focused to a spot of diameter <4 μm. Raman spectra were recorded in the range of 850–1950 cm^{-1}. After the performance of background noise subtraction, the spectra were deconvoluted by fitting two Gaussian distributions corresponding to *D* and *G* peaks associated with the in-plane bond-stretching vibration mode of sp^2 sites and the stretching and bending modes of sp^2 sites in the aromatic rings, respectively [21].

III. Results and Discussion

Figure 1 shows OSA images of laser-heated tracks on disks with different *a*-C films. The applied laser power increases from ~150 mW in the inner track of radius equal to 13 mm to ~300 mW in the outer track of radius equal to 16 mm. The contrast intensity correlates with the extent of changes in surface properties, with higher contrast implying more significant changes. The hardly distinguishable tracks corresponding to the lowest laser power (150 mW) suggest that changes in the surface properties of the *a*-C films, if any, were marginal. Significant changes in the film surface properties occurred for laser power >150 and >250 mW in the case of CVD and thin (~0.9 nm) FCVA films, respectively. However, changes in the surface properties of the thick (3.6 nm) FCVA film appear to be significantly less pronounced, indicating that the thick FCVA film is more thermally stable than the thin FCVA film, which itself is more stable than the much thicker CVD film.

Figure 2 shows typical Raman spectra of as-deposited *a*-C films, with characteristic *D* and *G* peaks centered at ~1350 and ~1550 cm^{-1}, respectively. The absence of a *D* peak from both FCVA film spectra reveals the existence of a high fraction of sp^3 hybridization in these films, resulting in limited amount of π bonding from aromatic rings. Alternatively, the presence of a *D* peak in the CVD film spectrum indicates the dominance of π bonding.

Figure 3 shows that laser heating affected the Raman spectrum of each film differently. Increasing the laser power (heating) changed significantly the spectrum of the CVD film [Fig. 3(*a*)]. However, the spectrum of the 3.6-nm-thick FCVA film [Fig. 3(*b*)] shows a secondary effect of laser heating on film structure, especially for laser power ≤250 mW, indicating a much higher thermal stability of *a*-C films deposited by FCVA. The 0.9-nm-thick FCVA film [Fig. 3(*c*)] shows significant changes at a laser power >250 mW. Since the *D* peak indicates the presence of aromatic rings and the *G* peak is mainly due to vibrations of all sp^2 sites in both chain and ring configurations, the increase in the *D* peak intensity indicates an increase in sp^2 sites [22]. Therefore, the *D*-to-*G* peak intensity ratio, $I(D)/I(G)$, can be used to obtain approximate estimates of the sp^3 fraction in the films.

The large shift of the *D* peak in the spectra of the *a*-C film deposited by CVD is associated with the conversion of sp^2 carbon configurations to less ordered aromatic rings. It is well known that visible Raman of laser wavelength equal to 514.5 nm is 50–200 times more sensitive to sp^2 than sp^3 hybridization due to the resonance effect of visible photons and sp^2 sites [23]. Therefore, the signal strength can be correlated with the amount of sp^2 hybridization. Consequently, the significant changes in the Raman spectra of the CVD film for laser power >150 mW and the thinner FCVA film for laser power >250 mW can be attributed to the evolution of sp^3-to-sp^2 transformation.

Figure 4(*a*) shows the effect of laser power (heating) on the *D*-to-*G* peak intensity ratio $I(D)/I(G)$, which may be indicative of the degree of carbon disorder in the film. As mentioned above, the *D* and *G* peaks were determined by deconvolution of the Raman spectra by Gaussian distributions [24]. Because the presence of C–H bonding in the CVD film complicates the interpretation based on the $I(D)/I(G)$ ratio, a comparison is made only for FCVA films. The higher $I(D)/I(G)$ of the as-deposited thin FCVA film indicates a relatively low sp^3 fraction. The sharp increase in $I(D)/I(G)$ of the CVD film for laser power >150 mW suggests a significant increase in the amount of disordered carbon, which may be related to carbon clustering. A correlation between *D*-peak intensity and degree of disordered carbon has been observed in *ab initio* Raman simulations [25]. The trend for $I(D)/I(G)$ to increase in the high laser power

range is much less pronounced for both FCVA films. Thus, the Raman results shown in Fig. 4(*a*) indicate that FCVA-synthesized *a*-C films exhibit much higher thermal stability than CVD films. In the case of the thin FCVA film, $I(D)/I(G)$ remains nearly constant for laser power >250 mW. This can be explained by considering the limited sp^3 bonding in the thin film and the presence of less carbon atoms that saturated the conversion to sp^2 bonding. The Raman results of the FCVA films reveal a decrease in thermal stability with decreasing film thickness. A plausible explanation for this trend is that, for a given laser power, the energy absorbed per carbon atom increases with the decrease of the film thickness.

Figure 4(*b*) shows the effect of laser heating on the *G*-peak position of CVD and FCVA films. It has been reported that a decrease in sp^3 fraction and the presence of a residual compressive stress can be correlated with an upward shift of the *G* peak [26,27]. In the present study, the *G* peak of the CVD film shows significant red-shifting, whereas that of the thicker FCVA film exhibits marginal variation due to laser heating. The slight changes in both the $I(D)/I(G)$ ratio and the *G*-peak position observed with the FCVA films are attributed to carbon bond stretching effects due to relaxation of the residual compressive stress in the films. The temperature rise in the laser-heated film enhances the carbon atom mobility, resulting in vigorous stretching of the atomic bonds, which, in turn, promotes residual stress relaxation and red-shifting of the *G* peak. Consequently, secondary changes in both $I(D)/I(G)$ and *G*-peak position may be attributed to restricted bond stretching. The Raman results indicate that laser heating altered the structure of the CVD film and the thin FCVA film through sp^3-to-sp^2 transformation and sp^2 clustering. Thus, laser heating at powers above 150 mW affected significantly the structure of the CVD film, contrary to FCVA films, which exhibited much higher thermal stability over the entire laser power range examined in this study (i.e., 250 mW and >300 mW for 0.9- and 3.6-nm-thick FCVA films, respectively).

The evolution of the film surface topography (roughness) during laser heating provides another means of exploring the thermal stability of the *a*-C films deposited by the two methods. Figure 5 shows the R_a roughness of CVD and FCVA films as a function of laser power. The thick FCVA film did not show any discernible changes in roughness and topography, conversely to the CVD and thin FCVA films

which were both roughened by laser heating, especially for laser power above a threshold level of 150 and 200 mW, respectively. The volume increase due to the extensive sp^3-to-sp^2 transformation [28] in the laser-heated CVD and thin FCVA films was restricted by the bulkier FePt substrate, resulting in a compressive residual stress in these films. Thus, the significant roughening of the CVD film for laser power >150 mW is attributed to carbon clustering induced by compressive stresses arising from atomic carbon rehybridization. The increased roughness of these *a*-C films increases the likelihood of intimate contact of the head with the disk surface and, in turn, the possibility of data loss due to surface damage. The results shown in Figs. 2–5 indicate that *a*-C films deposited by the CVD method are limited to EAMR heating conditions of laser power ≥150 mW, whereas FCVA-synthesized *a*-C films exhibit thermal stability up to higher laser powers, depending on the film thickness.

IV. CONCLUSIONS

The thermal stability of ultrathin *a*-C films synthesized by CVD and FCVA techniques was investigated by repetitively heating the films under different laser power conditions. Visible Raman spectroscopy showed that FCVA films possess superior thermal stability. CVD films exhibited atomic carbon rehybridization and structural change at laser powers >150 mW, whereas the thermal stability of FCVA films of similar thickness was not affected by laser heating even with the maximum laser power (300 mW) used in this study. Laser heating at powers >150 mW induced significant roughening of the CVD films, suggesting that *a*-C films synthesized by the CVD method are limited to EAMR conditions of relatively low laser power heating. FCVA films demonstrated a decrease in thermal stability with decreasing film thickness, which can be attributed to the higher thermal energy absorbed per carbon atom. The high thermal stability of *a*-C films synthesized by the FCVA method suggests that these films are prime candidate overcoats for EAMR hard disks.

ACKNOWLEDGMENTS

The authors are grateful to Y. Chen, Y. Sakane, and R. Hempstead from Western Digital Co., San Jose, California, for the technical support and the supply of hard disks. The first author (NW) would also like to acknowledge an internship during summer 2010 at Western Digital Co., San Jose, CA.

REFERENCES

[1] L. Pan and D. B. Bogy, "Heat-assisted magnetic recording," *Nature Photonics*, vol. 3, pp. 189–190, 2009.

[2] Z. Z. Bandić and R. H. Victora, "Advances in magnetic data storage technologies," *Proc. IEEE*, vol. 96, pp. 1749–1753, 2008.

[3] M. H. Kryder, E. C. Gage, T. W. McDaniel, W. A. Challener, R. E. Rottmayer, G. Ju, Y.-T. Hsia, and M. F. Erden, "Heat assisted magnetic recording," *Proc. IEEE*, vol. 96, pp. 1810–1835, 2008.

[4] J.-P. Wang, "FePt magnetic nanoparticles and their assembly for future magnetic media," *Proc. IEEE*, vol. 96, pp. 1847–1863, 2008.

[5] W. A. Challener, C. Peng, A. V. Itagi, D. Karns, W. Peng, Y. Peng, X. Yang, X. Zhu, N. J. Gokemeijer, Y.-T. Hsia, G. Ju, R. E. Rottmayer, M. A. Seigler, and E. C. Gage, "Heat-assisted magnetic recording by a near-field transducer with efficient optical energy transfer," *Nature Photonics*, vol. 3, pp. 220–224, 2009.

[6] B. C. Stipe, T. C. Strand, C. C. Poon, H. Balamane, T. D. Boone, J. A. Katine, J.-L. Li, V. Rawat, H. Nemoto, A. Hirotsune, O. Hellwig, R. Ruiz, E. Dobisz, D. S. Kercher, N. Robertson, T. R. Albrecht, and B. D. Terris, "Magnetic recording at 1.5 Pb m^{-2} using an integrated plasmonic antenna," *Nature Photonics*, vol. 4, pp. 484–488, 2010.

[7] C.-B. Rong, Y. Li, and J. P. Liu, "Curie temperatures of annealed FePt nanoparticle systems," *J. Appl. Phys.*, vol. 101, pp. 09K505(1–3), 2007.

[8] D. Wang, T. Seki, K. Takanashi, T. Shima, G. Li, H. Saito, and S. Ishio, "Dot size dependence of magnetization reversal process in $L1_0$-FePt dot arrays," *IEEE Trans. Mag.*, vol. 44, pp. 3464–3467, 2008.

[9] J.-I. Ikemoto, Y. Imai, and S. Nakagawa, "Control of Curie temperature of FePt(Cu) films prepared from Pt(Cu)/Fe bilayers," *IEEE Trans. Mag.*, vol. 44, pp. 3543–2546, 2008.

[10] N. Yasui, H. Inaba, K. Furusawa, M. Saito, and N. Ohtake, "Characterization of head overcoat for 1 Tb/in^2 magnetic recording," *IEEE Trans. Mag.*, vol. 45, pp. 805–809, 2009.

[11] D. S. Grierson, A. V. Sumant, A. R. Konicek, T. A. Friedmann, J. P. Sullivan, and R. W. Carpick, "Thermal stability and rehybridization of carbon bonding in tetrahedral amorphous carbon," *J. Appl. Phys.*, vol.107, pp. 033523(1–5), 2010.

[12] R. Kalish, Y. Lifshitz, K. Nugent, and S. Prawer, "Thermal stability and relaxation in diamond-like-carbon. A Raman study of films with different sp^3 fractions (*ta*-C to *a*-C)," *Appl. Phys.Lett.*, vol. 74, pp. 2936–2938, 1999.

[13] R. L. C. Wu, K. Miyoshi, R. Vuppuladhadium, and H. E. Jackson, "Physical and tribological properties of rapid thermal annealed diamond-like carbon films," *Surf. Coat. Technol.*, vol. 54/55, pp. 576–580, 1992.

[14] A. Grill, V. Patel, and B. S. Meyerson, "Optical and tribological properties of heat-treated diamond-like carbon," *J. Mater. Res.*, vol. 5, pp. 2531–2537, 1990.

[15] A. C. Ferrari, B. Kleinsorge, N. A. Morrison, A. Hart, V. Stolojan, and J. Robertson, "Stress reduction and bond stability during thermal annealing of tetrahedral amorphous carbon," *J. Appl. Phys.*, vol. 85, pp. 7191–7197, 1999.

[16] N. Tagawa and H. Tani, "Lubricant depletion characteristics induced by rapid laser heating in thermally assisted magnetic recording," *IEEE Trans. Mag.*, vol. 47, pp. 105–110, 2011.

[17] S. Anders, J. Díaz, J. W. Agger III, R. Y. Lo, and D. B. Bogy, "Thermal stability of amorphous hard carbon films produced by cathodic arc deposition," *Appl. Phys.Lett.*, vol. 71, pp. 3367–3369, 1997.

[18] H.-S. Zhang and K. Komvopoulos, "Direct-current cathodic vacuum arc system with magnetic-field mechanism for plasma stabilization," *Rev. Sci. Instrum.*, vol. 79, pp. 073905(1–7), 2008.

[19] H.-S. Zhang and K. Komvopoulos, "Synthesis of ultrathin carbon films by direct current filtered cathodic vacuum arc," *J. Appl. Phys.*, vol. 105, pp. 083305(1–7), 2009.

[20] H.-S. Zhang and K. Komvopoulos, "Surface modification of magnetic recording media by filtered cathodic vacuum arc," *J. Appl. Phys.*, vol. 106, pp. 093504(1–7), 2009.

[21] J. Robertson, "Diamond-like amorphous carbon," *Mater. Sci. Eng. R: Reports*, vol. 37, pp. 129–281, 2002.

[22] A. C. Ferrari and J. Robertson, "Interpretation of Raman spectra of disordered and amorphous carbon," *Phys. Rev. B*, vol. 61, pp. 14095–14107, 2000.

[23] S. Gupta, B. R. Weiner, W. H. Nelson, and G. Morell, "Ultraviolet and visible Raman spectroscopic investigations of nanocrystalline carbon thin films grown by bias-assisted hot-filament chemical vapor deposition," *J. Raman Spect*., vol. 34, pp. 192–198, 2003.

[24] F. C. Tai, S. C. Lee, J. Chen, C. Wei, and S. H. Chang, "Multipeak fitting analysis of Raman spectra on DLCH film," *J. Raman Spect*., vol. 40, pp. 1055–1059, 2009.

[25] C. Castiglioni, C. Mapelli, F. Negri, and G. Zerbi, "Origin of the *D* line in the Raman spectrum of graphite: A study based on Raman frequencies and intensities of polycyclic aromatic hydrocarbon molecules," *J. Chem. Phys.*, vol. 114, pp. 963–974, 2001.

[26] C. K. Chung, C. C. Peng, B. H. Wu, and T. S. Chen, "Residual stress and hardness behaviors of the two-layer C/Si films," *Surf. Coat. Technol.*, vol. 202, pp. 1149–1153, 2007.

[27] J.-K. Shin, C. S. Lee, K.-R. Lee, and K. Y. Eun, "Effect of residual stress on the Raman-spectrum analysis of tetrahedral amorphous carbon films," *Appl. Phys. Lett.*, vol. 78, pp. 631–633, 2001.

[28] C. A. Lucas, T. D. Nguyen, and J. B. Kortright, "X-ray reflectivity measurements of the expansion of carbon films upon annealing," *Appl. Phys. Lett.*, vol. 59, pp. 2100–2102, 1991.

List of Figures

Fig. 1 Optical surface analyzer measurements of repetitively heated tracks on *a*-C film surfaces for different laser powers: (*a*) 3.6-nm-thick CVD film, and (*b*) 3.6-nm-thick FCVA film, and (*c*) 0.9-nm-thick FCVA film.

Fig. 2 Visible Raman spectra of as-deposited CVD and FCVA *a*-C films. (The spectra have been shifted upward for clarity. Gaussian distributions corresponding to *D* and *G* peaks used to deconvolute the Raman spectra are shown in the spectrum of the CVD film.)

Fig. 3 Visible Raman spectra of *a*-C films obtained before and after heating at different laser powers: (*a*) 3.6-nm-thick CVD film, and (*b*) 3.6-nm-thick FCVA film, and (*c*) 0.9-nm-thick FCVA film. (The spectra have been shifted upward for clarity.)

Fig. 4 (a) *D*-to-*G* peak intensity ratio and (b) *G*-peak position of CVD and FCVA *a*-C films versus laser power. (Error bars are not shown for clarity. Typical standard deviations in (a) and (b) are equal to 0.013 and 8.2 cm^{-1}, respectively.)

Fig. 5 Surface roughness of CVD and FCVA *a*-C films measured with an AFM after heating at different laser powers.

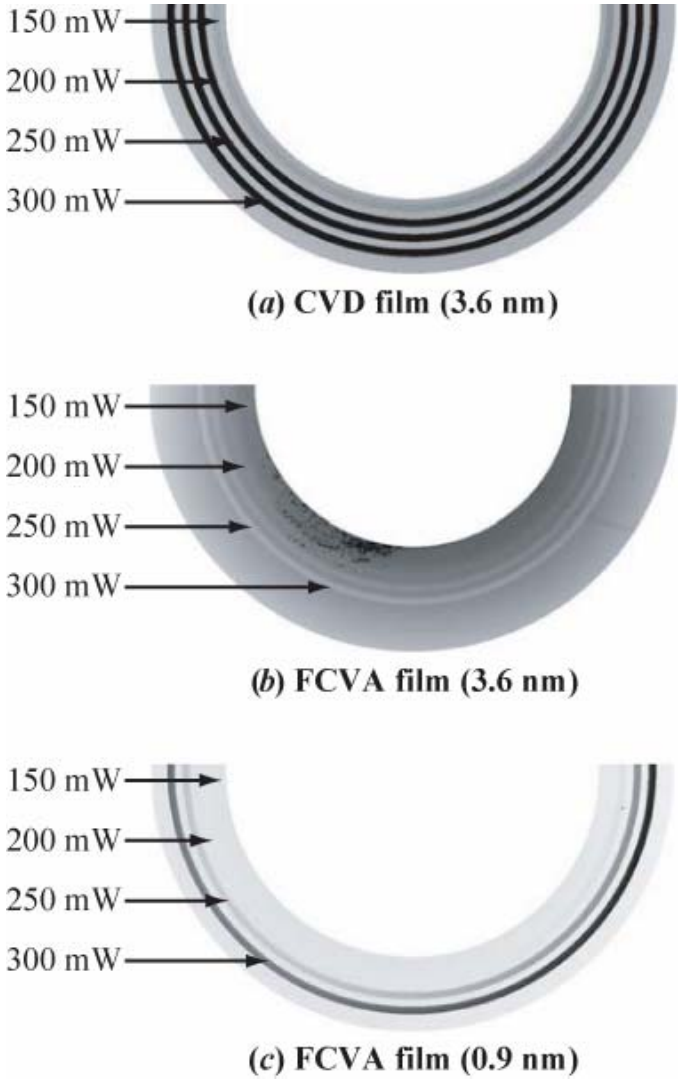
150 mW
200 mW
250 mW
300 mW
(a) CVD film (3.6 nm)
150 mW
200 mW
250 mW
300 mW
(b) FCVA film (3.6 nm)
150 mW
200 mW
250 mW
300 mW
(c) FCVA film (0.9 nm)

Figure 1

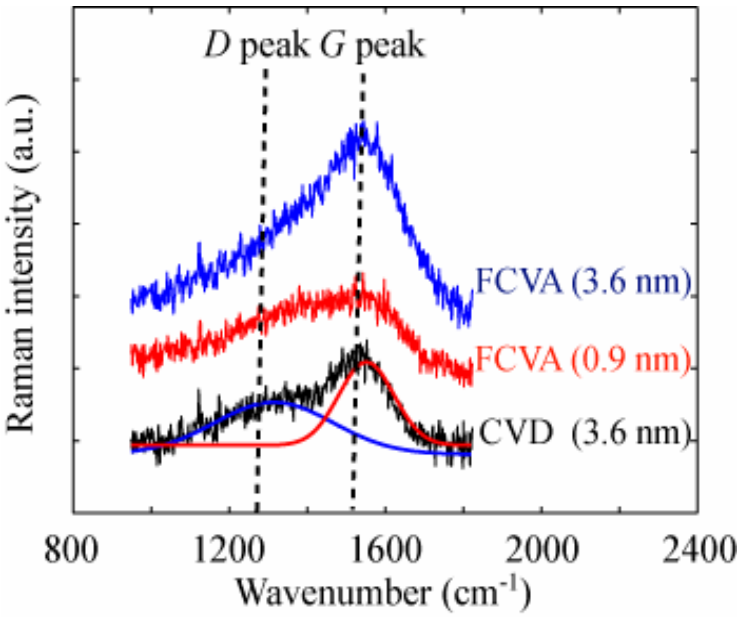
D peak G peak
Raman intensity (a.u.)
FCVA (3.6 nm)
FCVA (0.9 nm)
CVD (3.6 nm)
800
1200
1600
2000
2400
Wavenumber (cm-1)

Figure 2

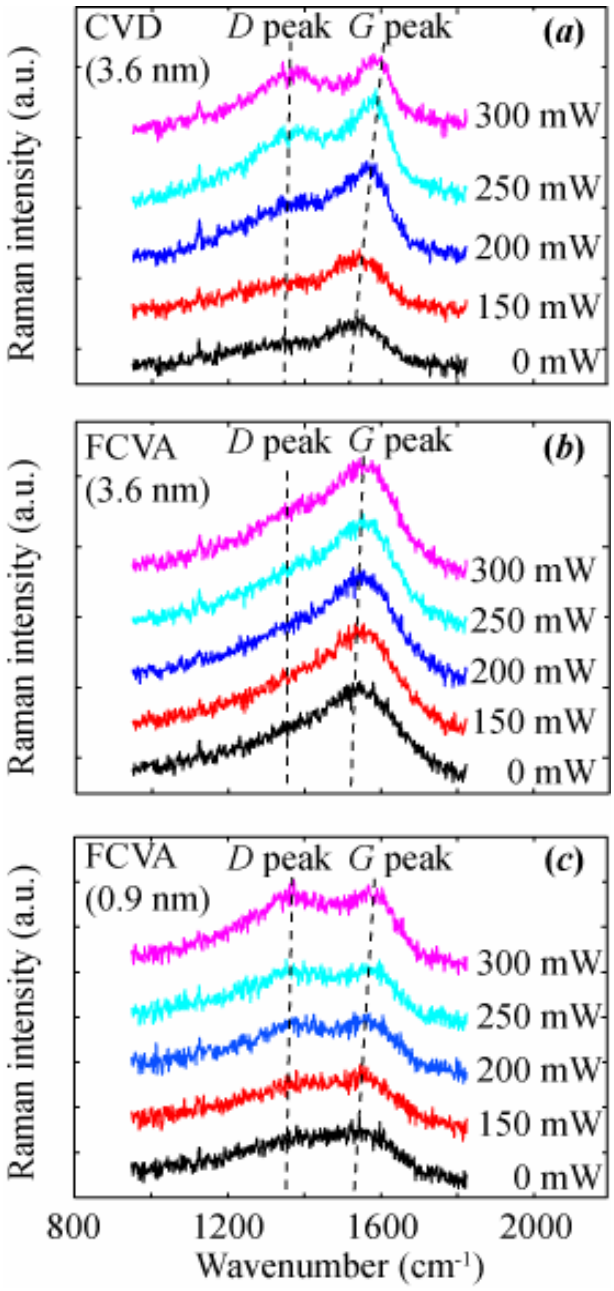
CVD
(3.6 nm)
D peak
G peak
(a)
300 mW
250 mW
200 mW
150 mW
0 mW
Raman intensity (a.u.)
FCVA
(3.6 nm)
D peak
G peak
(b)
300 mW
250 mW
200 mW
150 mW
0 mW
Raman intensity (a.u.)
FCVA
(0.9 nm)
D peak
G peak
(c)
300 mW
250 mW
200 mW
150 mW
0 mW
Raman intensity (a.u.)
800
1200
1600
2000
Wavenumber (cm-1)

Figure 3

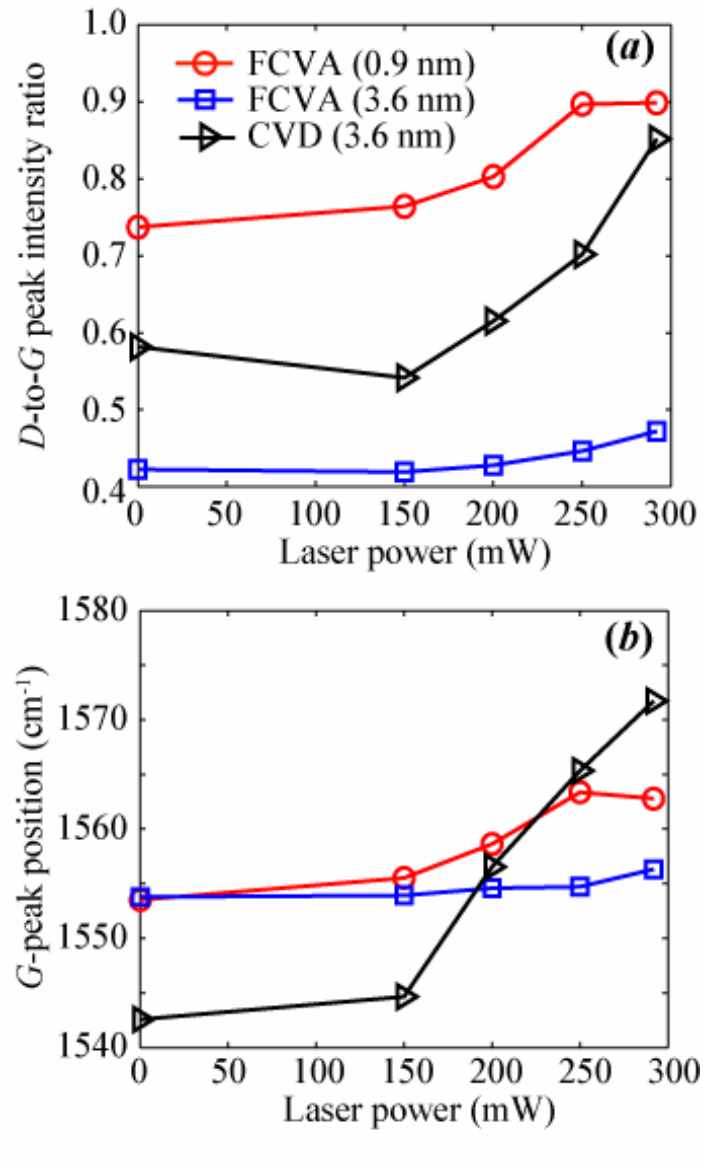
(a)
FCVA (0.9 nm)
FCVA (3.6 nm)
CVD (3.6 nm)
D-to-G peak intensity ratio
1.0
0.9
0.8
0.7
0.6
0.5
0.4
0
50
100
150
200
250
300
Laser power (mW)
(b)
G-peak position (cm-1)
1580
1570
1560
1550
1540
0
50
100
150
200
250
300
Laser power (mW)

Figure 4

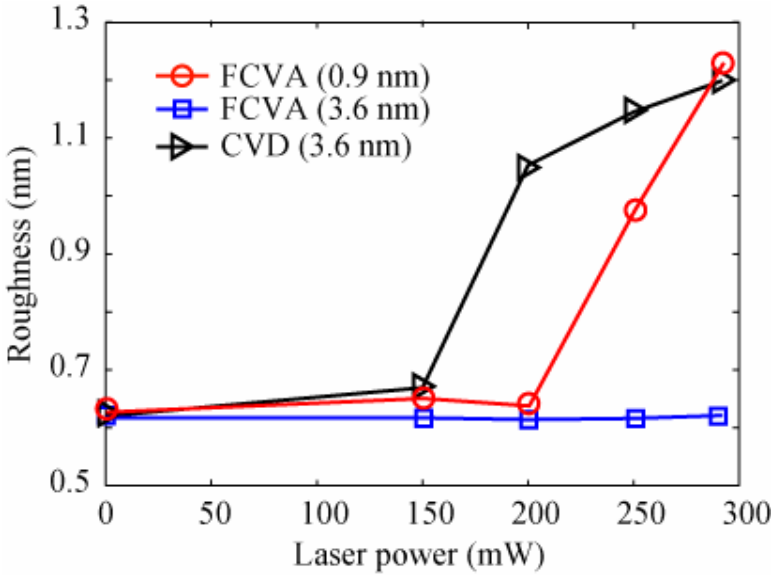
1.3
1.1
0.9
0.7
0.5
Roughness (nm)
0
50
100
150
200
250
300
Laser power (mW)
FCVA (0.9 nm)
FCVA (3.6 nm)
CVD (3.6 nm)

Figure 5